JOURNAL OF THERMOPHYSICS AND HEAT TRANSFER
Vol. 14, No. 4, October–December 2000

Passive Control of Convective Transport Phenomena Utilizing an Attached-Detached Rib-Array

Jenn-Jiang Hwang*
Chung-Hua University, Hsinchu 300, Taiwan, Republic of China
and
Chung-Hsin Chao†
Ta-Hwa Institute of Technology, Hsinchu 307, Taiwan, Republic of China

Passive control of heat transfer along a thermal boundary layer using an alternate attached-detached rib array is studied experimentally. Five clearance-to-rib height ratios ($c/h = 0$, 0.2, 0.4, 0.6, and 1.2) are examined in detail to compare their effects on the convective transport between two different rib spacings of $Pi/h = 5$ and 10. Results reveal that altering the rib clearance strongly affects the convective transport for $Pi/h = 5$, but negligibly for $Pi/h = 10$. For $c/h \geq 0.4$ the compound ribs for $Pi/h = 5.0$ have higher averaged heat transfer than those for $Pi/h = 10$, whereas a reversed trend is true for $c/h \leq 0.2$. In the case of $Pi/h = 5$, increasing c/h from 0.2 to 0.4 causes an abrupt jump in the averaged heat transfer and friction because of an alteration of turbulent transport, suggesting a critical rib clearance ratio between $c/h = 0.2$ and 0.4 for the transition of turbulent transport from the cavity flow to the separated-reattached flow together with vortex-shedding flow. In addition, lifting every other rib from the duct wall with $c/h = 0.4$ for $Pi/h = 5$ enhances the highest heat-transfer rate but also incurs the largest pressure-drop penalty. Correlations of averaged Nusselt number for the compound ribs of $Pi/h = 5$ are developed in terms of Reynolds number for different rib clearances for the first time.

Nomenclature

B	=	channel height
c	=	detached rib clearance
De	=	duct hydraulic diameter, $2B/(1 + B/W)$
f	=	friction factor
h	=	rib height
$\overline{Nu}$	=	local Nusselt number
$\overline{\overline{Nu}}$	=	averaged Nusselt number
$\overline{Nu}_s$	=	fully developed Nusselt number for smooth duct
Pi	=	rib pitch
Pr	=	Prandtl number
Re	=	Reynolds number, $U_b De/\nu$
T_b	=	local bulk mean temperature of air
T_w	=	local wall temperature
U_b	=	bulk velocity
u	=	streamwise fluctuation velocity
W	=	channel width
X	=	axial coordinate ($X = 0$ at the rib rear face)
X_s	=	axial coordinate ($X_s = 0$ at the duct entrance)
Y	=	transverse coordinate
Z	=	spanwise coordinate
ρ	=	air density
ν	=	air kinematic viscosity

Subscripts

b	=	bulk mean
s	=	smooth
w	=	wall

Introduction

FORCED convection over external boundaries in the presence of attached or detached ribroughness has constituted an important area of research for the past several decades because of the very fundamental and generic nature of this type of problem. In general, the convective transport over such a flow geometry is mainly governed by flow characteristics near the heat-transfer surface, i.e., the mean and/or turbulent velocities. For example, the attached ribs can break up the viscous sublayer and promote local wall turbulence that results in much higher heat transfer than can be obtained by flow over the smooth surface.[1–7] On the other hand, detaching the ribs from the heat-transfer surface with a clearance can enhance the local heat transfer on the smooth surface as a result of the accelerating flow through the gap and the vortex turbulence after the rib.[8–10] Recently, Tsia and Hwang[11] used compound rib arrays, namely, alternate attached-detached ribs (Fig. 1), to enhance heat transfer in a rectangular duct. Fluid flow and heat-transfer characteristics were measured under a fixed rib clearance to height ratio of $c/h = 0.5$ and three rib pitch to height ratios of $Pi/h = 10$, 20, and 30. A comparison of thermal performance was made among three kinds of ribbed walls, i.e., attached ribbed wall, detached ribbed wall, and alternate attached-detached ribbed wall. Results revealed that the compound ribbed geometry provided a little better performance than the surfaces roughened only with single type of ribs.

The main objective of this study is to extend the previous work[11] to investigate experimentally the effect of rib clearance on heat transfer and friction characteristics in the compound ribbed duct. A comparison of the rib-clearance effect on the convective transport is made between a narrow rib spacing of $Pi/h = 5$ and a wide rib spacing of $Pi/h = 10$. The physics and the relevance of altering the rib clearance for controlling the flow and temperature fields in the preceding cavity flow and reattached flow are discussed in detail, which has not been studied previously. Although, using compound ribs in industrial design is not yet practical because of manufacturing difficulties, it is important to understand the heat transfer and friction characteristics in a channel with compound ribs before an exact application is made. Moreover, the present data in conjunction with those from the previous work could provide a sound reference for computational-fluid-dynamic-based studies relating to heat transfer on a ribbed surface to assess the computation code and/or to evaluate the turbulence model.

Received 27 August 1999; revision received 1 June 2000; accepted for publication 5 June 2000.

*Professor, Department of Mechanical Engineering; jjhwang@chu.edu.tw.
†Assistant Professor, Department of Electrical Engineering.

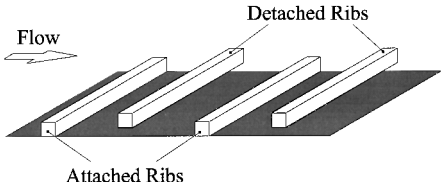

Fig. 1 Alternate attached-detached ribbed wall.

Experimental Apparatus

Apparatus

Detailed descriptions of the experimental apparatus have been provided in a previous paper,[12] and only some important features are stressed here again. The test channel is 1500 mm long and has a rectangular cross section of 160 mm (W) $\times$ 40 mm (B). The bottom duct wall is the heat-transfer surface roughened by a compound rib array, and the remaining three walls are smooth and thermally insulated. Twenty-two aluminum ribs of square cross section (10.4 $\times$ 10.4 mm) are, by turns, attached to and detached from the heated surface. The attached ribs are glued uniformly on the heated surface by thermal epoxy, whereas the detached ribs are placed over the heated surface with a clearance c and are screwed tightly from the channel side walls. A total of five rib clearances is tested, i.e., $c = 0$, 2.1, 4.2, 6.2, and 12.2 mm. Thermofoils (0.18 mm in thickness) are uniformly adhered between the stainless-steel sheet and the fiberglass board (6 mm in thickness) and are connected with dc power supplies for controllable electrical heating of the test channel. The fluid temperatures and heat-transfer coefficients on the floor of the ribbed wall are determined by using laser holographic interferometry (LHI),[13] whereas the mean and fluctuating velocities are measured by a hot-wire anemometer (DeltaLab) with normal I-type probe.[11] In addition, the flow structures in the compound ribbed duct are visualized by smoke injection under different rib clearances.[14] The preceding measurements are taken in the region between the 15th–17th ribs ($12 < X_s/De < 14$) from the duct entrance, where the thermal and hydraulic periodicities are achieved.[11] To measure the pressure drops across the compound ribbed channel, two pressure taps are located at the bottom channel wall after the 10th and 20th ribs, respectively. The pressure signals from each pressure tape are transferred to a micro-differential transducer and subsequently are amplified to a digital readout.

Data Analysis

The local Nusselt number on the heated wall deduced from the LHI can be presented as[13]

$$Nu = -\left(\frac{dT}{dY}\right)_w \frac{De}{(T_w - T_b)} \tag{1}$$

where the wall temperature gradient $(dT/dY)_w$ is determined by curve fitting, based on a least-squares method through the near-wall values of fluid temperature and fringe shift and T_w is read directly from the thermocouple output. Because significant uncertainties of local heat-transfer coefficient occur on the two rib flanks by using the LHI, the averaged Nusselt number $\overline{Nu}$ for the fully developed ribbed duct is determined by the energy balance methods,[11] rather than by integrating the local values along the wetted distance of the ribbed wall.

The friction factor of the periodically fully developed flow is calculated from the pressure drop across the test channel and the bulk velocity of the air, and it can be expressed as

$$f = \frac{[-(\Delta P/\Delta X) \cdot De]}{(\rho \cdot U_b^2/2)} \tag{2}$$

where the pressure gradient $\Delta P/\Delta X$ is evaluated by taking the ratio of the pressure difference and the distance of two pressure taps.

By using the uncertainty estimation method of Kline and McClintock,[14] the maximum uncertainties of local and averaged Nusselt numbers are estimated to be less than 8.9 and 7.4%, respectively, for Reynolds numbers larger than 8×10^3. The maximum uncertainty for f is estimated to be less than 7.3% for Reynolds numbers larger than 8×10^3. In addition, the individual experimental uncertainties for the measured physical quantities are $\pm 6.4\%$ for $T_w - T_b$, $\pm 5.6\%$ for ΔP, $\pm 2.4\%$ for U_b, and $\pm 8.2\%$ for $\sqrt{u^2}$.

Results and Discussion

Thermal Fluid and Flow Structures

Typical examples showing the effect of rib clearance to height ratio c/h on the isothermal patterns of the duct flows are given in Fig. 2. The corresponding flow structures visualized by smoke injection are shown in Fig. 3. The rib pitch-to-height ratio is fixed at $Pi/h = 5$, and the main flow with a fixed Reynolds number of $Re = 8 \times 10^3$ has a direction from left to right.

Figures 2a and 3a are the baseline case of a typical cavity flow. The results of detaching every other rib from the wall with a small rib clearance of $c/h = 0.2$ are shown in Figs. 2b and 3b. Comparing the results of Figs. 2a and 2b reveals that the fringe patterns around the attached ribs for $c/h = 0$ and 0.2 are largely similar. However, differences are clearly observed for the fringes behind the detached ribs and those behind the attached ribs. First, the fluid temperature behind the attached ribs decreases from the rib base to the rib top, whereas the fluid temperature gradient along the Y direction of the detached rib is relatively small; roughly, the detached rib is isothermal. Then, the fluid temperature near the rear face of the attached rib decreases along the X direction. However, the detached rib has a positive fluid temperature gradient in X direction behind the ribs, indicating a heat flow from fluid to the detached rib. This is because no fluid passes through the gap beneath the detached rib for $c/h = 0.2$, and thus the fluid within the gap is nearly stagnant, which acts as an adiabatic film to prevent heat conducted from the duct wall into the detached ribs. The detached ribs therefore act as thermally inactive ribs mounted above the heated wall.[15] Consequently, heat is totally convected from the duct wall. This results in a rather high fluid temperature above the duct wall just behind the detached rib. In the case of attached ribbed wall ($c/h = 0$), however, heat from the duct wall can be easily routed into the conducting attached

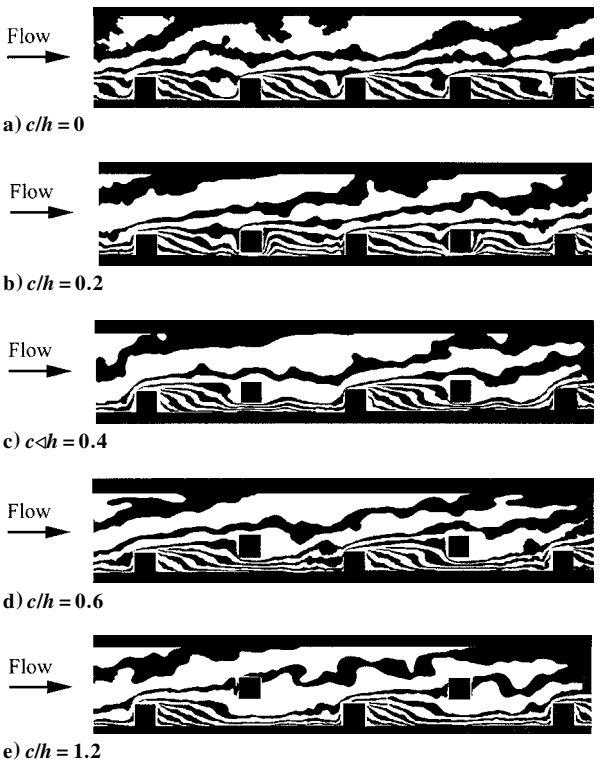

Fig. 2 Typical examples of the interferograms for the compound ribbed walls under $Re = 8 \times 10^3$.

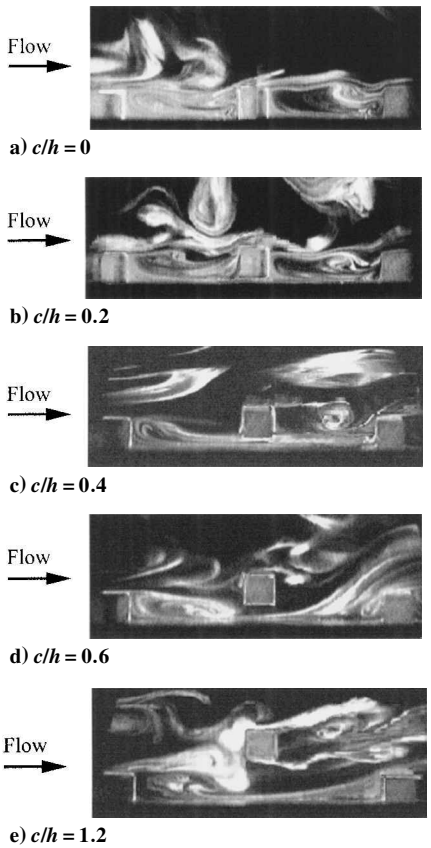

Fig. 3 Smoke-injection flow visualizations of the compound ribbed duct flows under $Re = 8 \times 10^3$.

rib and then is removed from the rib surfaces to the coolant by convection.

When c/h increases to =0.4 (Fig. 2c), the fluid-temperature distributions are significantly different from those for $c/h = 0$ and 0.2, especially around and behind the detached rib. In the case of $c/h = 0.4$, the gap beneath the detached rib is large enough to allow the fluid to penetrate, and thus the fluid within the cavity is no longer "dead" (Fig. 3c). In addition, the separated flow from the top of the attached rib reattaches to the duct wall rather than to the detached rib as in the case of $c/h = 0.2$. The reattached flow then develops and goes through the gap beneath the detached rib. Meanwhile, the separated flow from the upstream corner of the detached rib sheds downstream and mixes with jet emitting from the rib gap. To summarize, the flow transport just mentioned includes flow separation, reattached flow, redeveloping flow, recirculated flow, shedding vortices, and wall jets. When the rib clearance further increases to $c/h = 0.6$ (Fig. 2d), the thermal boundary layer beneath and behind the detached rib becomes thick because the flow acceleration effect is weakened (Fig. 3d). As for the highest rib clearance ($c/h = 1.2$, Fig. 2e and 3e), the detached rib seems to have an insignificant effect on the isotherm structures near the duct wall.

Local Heat-Transfer Distributions

Distributions of the local Nusselt number ratio $Nu/\overline{Nu}_s$ along the duct axis X/h for various c/h values are presented in Fig. 4, where $\overline{Nu}_s = 0.023 Re^{0.8} Pr^{0.4}$ is the fully developed Nusselt number for smooth ducts. The rib spacing and height are fixed at $Pi/h = 5$ and $h/B = 0.26$, respectively. The previous results (dashed line) of the attached-ribbed wall for $Pi/h = 10$ (Ref. 16) are also plotted for comparison.

For $c/h = 0$ (center line) the $Nu/\overline{Nu}_s$ ratio starts with a local minimum from the cavity floor after the attached rib, then increases along the axial distance, and finally decreases before approaching the next attached rib. For the small rib clearance of $c/h = 0.2$, the $Nu/\overline{Nu}_s$ distributions around and behind the detached rib, i.e., from $X/h = 3.0$ to 6.0, are rather different from those for $c/h = 0$. Beneath the detached rib the heat-transfer coefficient is very small as a result of the stagnant fluid (i.e., without force convection). The lower rate of wall heat transfer ahead of the detached rib ($X/h = 3.0$–4.0) than that of the attached ribs is because of the smaller fin effect for $c/h = 0.2$. When the rib clearance increases to $c/h = 0.4$, the local heat-transfer coefficient on the wall increases with increasing axial distance. A notable bump of the $Nu/\overline{Nu}_s$ distribution at the location beneath the detached rib is attributed to the effect of flow acceleration through the rib gap. This bump becomes less significant as the value of c/h further increases beyond $c/h = 0.4$ because the flow acceleration effect is gradually reduced. The values of $Nu/\overline{Nu}_s$ for $c/h \geq 0.4$ are higher than those of the wall mounted with an array of attached ribs with $Pi/h = 10$ (dashed line; Ref. 16), especially behind the detached rib. This is very reasonable because in respect to the earlier attached-ribbed wall of $Pi/h = 10$ the present compound ribbed wall has an additional detached rib between the two attached ribs. This mid-detached rib not only creates a jet-like flow beneath and behind the detached ribs but also acts as a turbulence promoter to enhance more heat transfer from the wall.

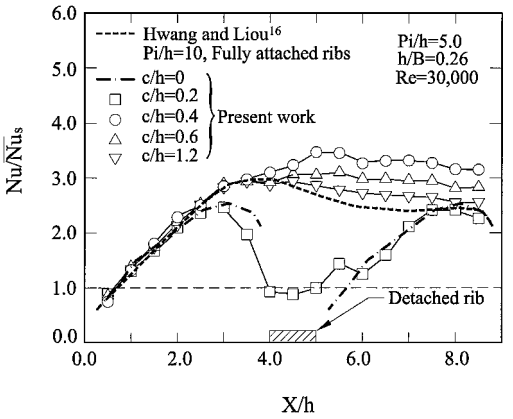

Fig. 4 Local Nusselt-number distributions on the floor of the compound ribbed walls.

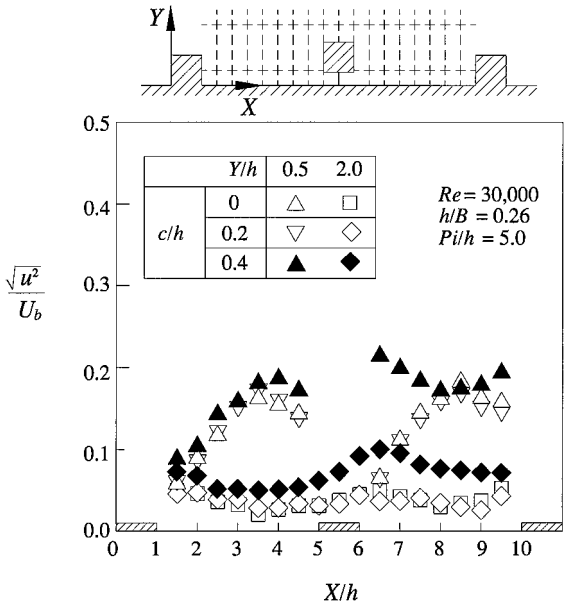

Fig. 5 Turbulence intensity distributions along the streamwise directions of $Y/h = 0.5$ and 2.0.

To provide a more rationale of the local heat-transfer augmentation, the turbulence-intensity characteristics are required, in addition to the mean flow structures visualized in Fig. 3. Figure 5 shows the distributions of turbulence intensity $\sqrt{(u^2)}/U_b$ along the channel centerline ($Z = 0$) for two elevations, i.e., $Y/h = 0.5$ and 2.0. The distributions of $\sqrt{(u^2)}/U_b$ for $c/h = 0$ and 0.2 are almost the

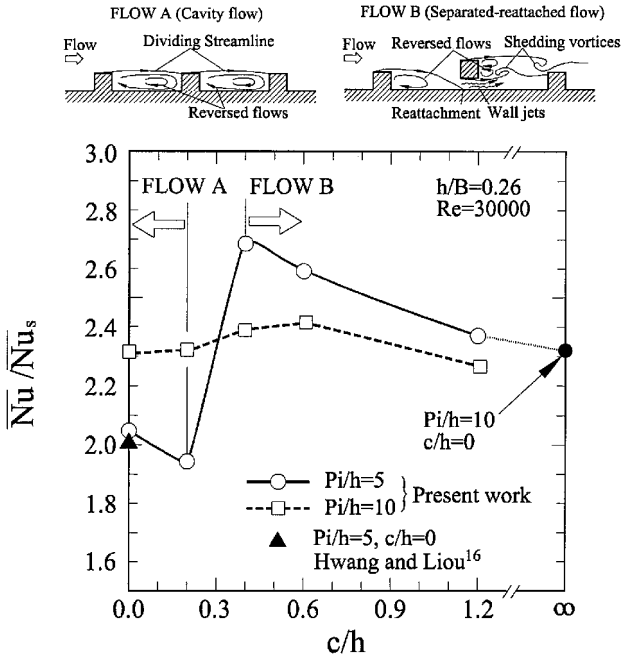

Fig. 6 Effect of rib clearance on the averaged Nusselt number.

same. But they are quite different from those of $c/h = 0.4$. Along the elevation of $Y/h = 0.5$ for $c/h = 0$ and 0.2, the $\sqrt{(u^2)}/U_b$ distribution reveals a well-known trend,[14] i.e., it begins with a local minimum, increases to a local maximum, near the midplane between the ribs, and then decreases slightly before encountering the next rib. For $c/h = 0.4$ the $\sqrt{(u^2)}/U_b$ distribution along the ribbed wall begins with a local minimum and increases to a local maximum at $X/h = 4.0$ because of the flow reattachment. Then, another maximum appears behind the detached rib ($X/h = 5.5$) caused by the strong turbulent transport by a wall-jet flow emitting from the gap beneath the rib. Globally, the values of $\sqrt{(u^2)}/U_b$ for $c/h = 0.4$, both for the near-wall and the core-flow regions, are higher than those for $c/h = 0$ and 0.2. In addition, the $\sqrt{(u^2)}/U_b$ distributions are consistent with the flow structures shown in Fig. 3, and both of which give a reasonable explanation of the local heat-transfer distributions described earlier.

Averaged Nusselt Number

Typical results illustrating the effect of rib clearance ratio c/h on the averaged Nusselt number ratio $\overline{Nu}/\overline{Nu}_s$ for $Pi/h = 5$ and 10 are shown in Fig. 6. The earlier results for the wall roughened by attached ribs with $Pi/h = 5$ (solid symbols, Ref. 16) are also displayed for comparison. Attention is first focused on the results for the narrow rib spacing, i.e., $Pi/h = 5$. As shown in Fig. 6, the $\overline{Nu}/\overline{Nu}_s$ starts with a relatively low value at $c/h = 0$, slightly decreases to a local minimum at $c/h = 0.2$, then sharply increases to a local maximum at $c/h = 0.4$ and decreases gradually, and finally approaches a constant value as c/h further increases. The first decrease of $\overline{Nu}/\overline{Nu}_s$ from $c/h = 0$ to 0.2 is mainly caused by the vanishing of the fin effect for $c/h = 0.2$, whereas the sharp increase between $c/h = 0.2$ and 0.4 is attributed to an alteration in fluid-flow mechanisms. In the case of $c/h = 0.4$, the gap beneath the detached rib is high enough to be permeable, thus forming complex flow structures of FLOW B, Fig. 6. The abrupt change in the $\overline{Nu}/\overline{Nu}_s$ distribution suggests the existence of a critical clearance ratio between $0.2 < c/h < 0.4$ above which the heat transfer from the duct wall is significantly enhanced by FLOW B. On the other hand, when c/h is below the critical value, a flow reversal occupies the entire cavity (FLOW A, Fig. 6), and the heat cannot be removed as much from the wall as that by FLOW B. When $c/h > 0.4$, a slight decrease in $\overline{Nu}/\overline{Nu}_s$ with increasing c/h is caused by a decrease in the strength of the jet-like flow as well as by the vortex-shedding effect on the duct wall. When c/h further increases, as expected, the

Table 1 Coefficients of heat-transfer correlations in Eq. (3)

	$\overline{Nu} = aRe^b$		
c/h	a	b	Maximum error, %
0	0.232	0.626	3.8
0.2	0.231	0.626	5.3
0.4	0.321	0.628	8.1
0.6	0.298	0.630	4.3
1.2	0.284	0.624	5.8

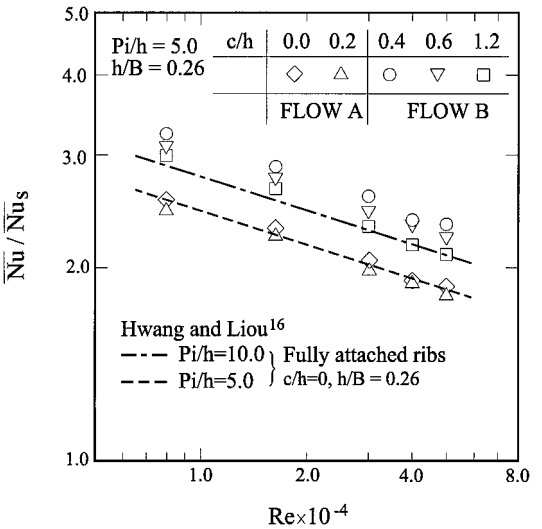

Fig. 7 Reynolds-number dependence of averaged Nusselt number for various rib clearances.

averaged Nusselt number approaches the value for $c/h = \infty$ (solid circle). In fact, this limiting value is for the data with $c/h = 0$ and $Pi/h = 10$. As can be seen from Fig. 6, the effect of c/h on $\overline{Nu}/\overline{Nu}_s$ is insignificant for $Pi/h = 10$. This is because the convective transport does not change too much for the reattached flow by lifting every other rib from the duct wall with a clearance. The wall heat transfer for the compound ribs with $Pi/h = 5.0$ for $c/h \geq 0.4$ is in excess of that for $Pi/h = 10$. This trend is reversed for $c/h \leq 0.2$.

Figure 7 shows the Reynolds-number dependence of $\overline{Nu}/\overline{Nu}_s$ for various rib clearances. The dashed and centerlines shown in this figure are the previous results[16] of the wall mounted with attached ribs for $Pi/h = 5$ and 10, respectively. As can be observed from this figure, the values of $\overline{Nu}/\overline{Nu}_s$ for the compound ribbed walls decrease with increasing Reynolds number. The preceding correlation for the $Pi/h = 5$ case (dashed line) represents well the present data for $c/h = 0$ and 0.2. In addition, the heat transfer augmented by FLOW B ($c/h \geq 0.4$) is higher than that by FLOW A and is even higher than that of the reattached flow with $Pi/h = 10$. The extent in the heat transfer enhancement by lifting every other rib from the duct wall with a clearance of $c/h = 0.4$ is up to 35% for $Pi/h = 5$. The present data for the compound ribbed walls of various rib clearances, as shown in Fig. 7, can be correlated in the form

$$\overline{Nu} = aRe^b \tag{3}$$

The values of a and b for the five different rib clearances are listed in Table 1. The maximum deviation in $\overline{Nu}$ between the preceding equations and the experimental data shown in Fig. 7 is less than 5.3%.

Friction Factors

Figure 8 shows the Reynolds-number dependence of friction factor under various rib clearances. The earlier results for the attached-rib flow[16] and the smooth-duct flow are displayed for comparison. The friction factors for $c/h = 0$ and 0.2 are almost the same as a result of the similar fluid-flow mechanisms (FLOW A). For $c/h \geq 0.4$ FLOW B creates not only a steeper expansion and contraction of the stream tube as a result of the presence of reattachment but also the vortex shedding from the mid-detached rib, and hence it gives rise to

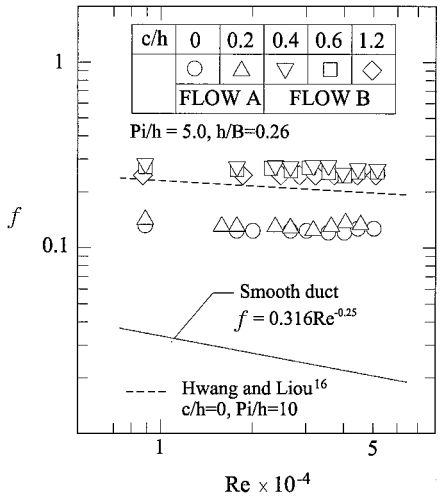

Fig. 8 Reynolds-number dependence of friction factor for various rib clearances.

a greater value of f. As compared to the smooth duct results, the increase in pressure-droppenalties is about 4.2–7.8 times for FLOW A and 6.0–12.5 times for FLOW B. As far as constant-pumping-power performance is concerned, a 35% increase in heat-transfer rate penalized by a 70% increase in pressure drop for the present compound ribs with $c/h \geq 0.4$ is acceptable.[15] It is further seen from this figure that the friction factors for $c/h \geq 0.4$ are slightly higher than those for attached ribs with $Pi/h = 10$ (Ref. 16) because the case of $Pi/h = 5$ for $c/h \geq 0.4$ can be regarded as the geometry that places an additional detached rib array on the attached ribbed geometry with $Pi/h = 10$.

Conclusions

Passive alteration of heat transfer on a heated wall using alternate attached-detached ribs has been studied experimentally. The effect of the governing parameter c/h is explored in detail. A comparison of c/h effect between two different rib spacings of $Pi/h = 5$ and 10 is made. The key finding of the present work is the existence of a critical clearance to height ratio c/h between 0.2 and 0.4 for $Pi/h = 5$, with regard to its effect on the rapid changes in heat transfer and pressure drop. This phenomenon is not found for a wide rib spacing of $Pi/h = 10$. Additional findings include the following:

1) In the case of $Pi/h = 5$, altering the rib clearance strongly affects the heat-transfer characteristics of the ribbed wall through modifying the fin effect and/or the turbulence transport. However, the rib clearance effect is insignificant for $Pi/h = 10$.

2) The averaged heat-transfer coefficient for the compound ribs with $Pi/h = 5.0$ for $c/h \geq 0.4$ is higher than that with $Pi/h = 10$. The trend is reversed for $c/h \leq 0.2$.

3) For $Pi/h = 5$ the compound ribs with c/h below the critical value have a reversed boundary layer occupying the entire cavity between consecutive ribs (FLOW A), which yields a relatively low heat transfer. On the contrary, as long as c/h is larger than the critical value, the compound ribs can enhance a much higher heat transfer through complex turbulence transport of reattaching flow together with vortex shedding and wall-jet flow (FLOW B).

4) The compound ribs of $c/h = 0.4$ for $Pi/h = 5$ perform with the best heat-transfer coefficient, with an enhancement of up to 35% as compared to the results for $c/h = 0$. Meanwhile, the penalty in pressure drop is also the largest, typically about 70% higher than the results for $c/h = 0$.

5) Correlations for averaged Nusselt number for the compound ribs of $Pi/h = 5$ are developed in terms of Reynolds number for different rib clearances for the first time.

Acknowledgment

This work was sponsored by the National Science Council of Taiwan (ROC), under Contract NSC 85-2212-E-216-003.

References

[1] Burggraf, F., "Experimental Heat Transfer and Pressure Drop with Two-Dimensional Discrete Turbulence Promoters Applied to Two Opposite Walls of a Square Tube," *Augmentation of Convective Heat and Mass Transfer*, edited by E. E. Bergles and R. L. Webb, American Society of Mechanical Engineers, New York, 1970, pp. 70–79.

[2] Webb, R. L., and Eckert, E. R. G., "Application of Rough Surfaces to Heat Exchanger Design," *International Journal of Heat and Mass Transfer*, Vol. 15, No. 6, 1972, pp. 1647–1658.

[3] Sparrow, E. M., and Tao, W. Q., "Enhanced Heat Transfer in a Flat Rectangular Duct with Streamwise-Periodic Disturbances at One Principal Wall," *Journal of Heat Transfer*, Vol. 105, No. 4, 1983, pp. 851–861.

[4] Han, J. C., "Heat Transfer and Friction Characteristics in Rectangular Channels with Rib Turbulators," *Journal of Heat Transfer*, Vol. 110, No. 2, 1988, pp. 321–328.

[5] Chyu, M. K., and Wu, L. X., "Combined Effects of Rib Angle-of-Attack and Pitch-to-Height Ratio on Mass Transfer from a Surface with Transverse Ribs," *Experimental Heat Transfer*, Vol. 2, No. 2, 1989, pp. 291–308.

[6] Acharya, S., Dutta, S., Myrum, T. A., and Baker, R. S., "Turbulent Flow Past a Surface-Mounted Two-Dimensional Rib," *Journal of Fluids Engineering*, Vol. 116, No. 2, 1993, pp. 238–246.

[7] Hwang, J. J., "Turbulent Heat Transfer and Fluid Flow in a Porous-Baffled Channel," *Journal of Thermophysics and Heat Transfer*, Vol. 11, No. 3, 1997, pp. 429–436.

[8] Kawaguchi, Y., Suzuki, K., and Sato, T., "Heat Transfer Promotion with a Cylinder Array Located near the Wall," *International Journal of Heat and Fluid Flow*, Vol. 6, No. 4, 1985, pp. 249–255.

[9] Oyakawa, K., Shinzato, T., and Mabuchi, I., "Effect of Heat Transfer Augmentation of Some Geometric Shapes of a Turbulence Promoter in a Rectangular Duct," *Bulletin of the Japan Society of Mechanical Engineers*, Vol. 29, No. 4, 1986, pp. 3415–3420.

[10] Yao, M., Nakatani, M., and Suzuki, K., "An Experimental Study on Pressure Drop and Heat Transfer in a Duct with a Staggered Array of Cylinders," *Proceedings of ASME-JSME Thermal Engineering Joint Conference*, Vol. 5, 1987, pp. 189–196.

[11] Tsia, Y. P., and Hwang, J. J., "Measurements of Heat Transfer and Fluid Flow in a Rectangular Duct with Alternate Attached-Detached Rib-Arrays," *International Journal of Heat and Mass Transfer*, Vol. 42, No. 1, 1999, pp. 2071–2083.

[12] Hwang, J. J., and Lai, D. Y., "Three-Dimensional Laminar Flow in a Rotating Multiple-Pass Square Channel with Sharp 180-Deg Turns," *Journal of Fluids Engineering*, Vol. 120, No. 3, 1998, pp. 488–495.

[13] Hwang, J. J., and Liou, T. M., "Heat Transfer in a Rectangular Channel with Perforated Turbulence Promoters Using Holographic Interferometry Measurement," *International Journal of Heat and Mass Transfer*, Vol. 38, No. 17, 1995, pp. 3197–3207.

[14] Kline, S. J., and McClintock, F. A., "Describing Uncertainties on Single-Sample Experiments," *Mechanical Engineering*," Vol. 57, No.1, 1953, pp. 3–8.

[15] Hwang, J. J., "Heat Transfer-Friction Characteristic Comparison in Rectangular Ducts with Slit and Solid Ribs Mounted on One Wall," *Journal of Heat Transfer*, Vol. 120, No. 3, 1998, pp. 709–716.

[16] Hwang, J. J., and Liou, T. M., "Augmented Heat Transfer in a Rectangular Channel with Permeable Ribs Mounted on the Wall," *Journal of Heat Transfer*, Vol. 116, No. 4, 1994, pp. 912–920.